doi:10.3788/gzxb20154410.1022001

用于超分辨成像的光瞳滤波器加工质量与性能参量分析

吕罗兰,张祥朝,徐敏

(复旦大学 上海超精密光学制造工程技术研究中心,上海 200438)

摘 要:用 Spearman 相关度分析法研究了 3 环带纯相位光瞳滤波器的加工质量与超分辨性能之间的显著度关系,并比较了不同环带光瞳滤波器的偏心对超分辨性能的影响.结果表明,环带的偏心与光斑半径、Strehl 比的相关度系数均大于 0.8,倒圆可使一级旁瓣强度的变化率高达 29.04%,因此环带偏心和倒圆是决定元件性能的有效表面质量参量;外层环带偏心对超分辨性能的影响大于内层环带,需要更加严格的公差控制.该方法为微光学元件设计加工中的准确度控制提供了理论依据及可行的技术途径.

关键词:微光学元件;加工误差;性能参量;光瞳滤波器;超分辨成像;公差控制;相关系数

中图分类号:TH742 **文献标识码**:A **文章编号**:1004-4213(2015)10-1022001-7

Analysis of Geometrical Qualities and Functionalities of Pupil-filters Used for Super-resolution Imaging

LÜ Luo-lan, ZHANG Xiang-chao, XU Min

(*Shanghai Engineering Centre of Ultra-Precision Optical Manufacturing, Fudan University, Shanghai* 200438, *China*)

Abstract: The Spearman's correlation coefficients between various fabrication errors and functionalities were analyzed on a 3-belt phase-only pupil-filter. Three kinds of pupil-filters with different numbers of belts were compared to identify the influence of eccentricities of different belts. The correlation coefficients between eccentricity and the radius at half central intensity and Strehl ratio are both greater than 0.8, and rounding can cause the intensity of the first order sidelobe changing up to 29.04%, thus these two parameters are identified as the significant geometrical parameters. Besides, the eccentricities of outer belts affect the super-resolution performance more significantly than inner belts, therefore they need to be controlled with tighter tolerances. This method provides a theoretical foundation and a versatile technical route for the effective specification in design and manufacturing of micro-optical elements.

Key words: Micro-optics; Fabrication error; Functionalities; Pupil-filter; Super-resolution imaging; Tolerance control; Correlation coefficient

OCIS Codes: 220.4000; 240.3990; 130.3990; 110.0180

Foundation item: The National Natural Science Foundation of China (No. 51205064), Shanghai Natural Science Foundation (No. 12ZR1441100) and Open Fund of CAEP (No. KF14004)

First author: LÜ Luo-lan (1992—), female, M. S. degree candidate, mainly focuses on modeling of micro-optics. Email:13210720011@fudan.edu.cn

Responsible author(Corresponding author): ZHANG Xiang-chao (1982—), male, associate professor, Ph. D, mainly focuses on surface metrology and optical measurement technology. Email:zxchao@fudan.edu.cn

Received: May. 03, 2015; **Accepted**: Jun. 17, 2015

0 Introduction

Dating from the 1960s, with the advent of laser, it has been witnessed that micro-optics, featured in the micrometer to nanometer range, are increasingly encroaching in the modern technical domain[1]. In most cases, the functionalities of micro-optics, like diffraction[2] are realized via the intricate micro-structures on the functional surfaces.

At present, the surface specifications for geometrical parameters standardized in ISO 25178-2: 2012[3] etc are based on traditional stochastic surfaces, describing the statistical properties of some overall textures (e. g. roughness, waviness and form error) and neglecting the effect of individual features. As micro-optical elements are manufactured with micro-fabrication technology, the micro-structures (e. g. binary steps and pyramids) contain some sharp features and steep slopes; hence they are very difficult to be measured. While verifying the functional behavior, in most cases the performance of the workpiece is compared to a nominal shape to examine whether the design targets are fulfilled. This approach cannot provide reliable information about the quality of the element. Moreover, the diversities in micro-optics and their functionalities make it challenging to develop a universal guideline for the specifications of geometrical parameters and their tolerances. Thereby the lack of information concerning the correlation between the geometrical qualities and functionalities results in the blindness in choosing surface parameters and setting tolerances in the design process. The fabrication difficulty and cost will in turn be increased factitiously. Hence, a new quality control procedure needs to be established in a function-oriented way to ensure the reliable inter-relationship between the geometrical specifications and functional properties. The pupil-filter structured in binary reliefs is a typical micro-optical element used to realize super-resolution imaging. Luo et al[4] have demonstrated that a phase pupil-filter achieves better super-resolution performance than amplitude pupil-filter. Zhao et al.[5] investigated the fabrication errors of several structural parameters. However, the calculation was based on the assumption that the Point Spread Function (PSF) of the imaging system is symmetrical, which is obviously not reliable. Liu et al.[6] investigated the influence of different intensity profiles of Gaussian beam on the super-resolution performance, but the dimensional parameters of the pupil-filter were not considered. Weckenmann and Hartmann[7-9] proposed a method to define geometrical parameters with the intended function based on a parameterized mathematical-physical model. This method defines geometrical parameters in a function-oriented way and makes the functionalities quantitatively predictable.

1 Identification of effective geometrical parameters of micro-optics

The target of understanding the correlation between topographies and functional performance is not only to ensure the significance of dimensional parameters, but also to develop a standardized quality control procedure which empowers the communication for engineers. The proposed method is composed of five steps, as below.

1.1 Definition of surface quality parameters

The geometrical parameters to be defined depend on the particular shapes and fabrication processes of the elements. It should be noticed that the featured structures on the surfaces by which the element achieves its functionality need to be recognized primarily. For the extreme complication in topography, the micro-morphologies can be divided into various classes of fabrication errors according to scales and shapes which will in turn influence different functionalities pertinently. With more comprehensive knowledge about the manufacturing of particular micro-optics, the fabrication errors can be modeled more reasonably. As a consequence sufficient geometrical parameters should be considered to cover all the structural features on the surfaces.

1.2 Identification of functional parameters

The functional parameters can be defined based on the practical applications, like the homogeneity of light patterns for beam shaping, or the aberration for optical imaging. Besides the functionalities should be distinguished according to their degree of importance.

1.3 Simulation of functional performance

Before simulation, an optimal system should be established, and the variations of geometrical parameters should accord with practical fabrication. Then the actual optical performance of the elements added with various fabrication errors can be calculated. It is worth mentioning that appropriate approximation should be conducted on the mathematical-physical model to get a balance between the calculation costs and modeling accuracy in the simulation analysis.

1.4 Analysis of correlations

This step is aimed to investigate the quantitative interrelationship between the geometrical parameters and functionalities. Based on the simulation results, the Spearman′s correlation coefficients between the fabrication errors and functional properties can be analyzed. The correlation coefficients are classified into 5 levels to assess the degree of dependence between

different parameter pairs[10]. More importantly, this method can be applied for multi-factor analysis.

1.5 Determination of significant parameters

According to Spearman′s rank correlation coefficients matrix, the geometrical parameters that significantly influence the functionalities will be determined. Then a set of significant quality parameters which can effectively control the actual performance of the micro-optical elements is identified for the designers and to avoid over-tight tolerances.

2 The pupil-filter used for super-resolution imaging

Super-resolution means that the spot size of the PSF of an optical system is beyond the diffraction limit. According to Rayleigh criterion[11], the two separated objects in an image can be distinguished by human eyes when the contrast factor is $K=15\%$. K is expressed as

$$K=\frac{I_{\max}-I_{\min}}{I_{\max}+I_{\min}}$$

and the minimum resolvable distance is expressed as

$$\sigma=1.22\frac{\lambda f}{D} \tag{1}$$

where $I_{\max}$ and $I_{\min}$ are the maximum and minimum intensities, respectively, λ is the wavelength, f is the focal length of the objective, and D is the diameter of the lens′ aperture. The pupil-filter provides a solution to achieve super-resolution. It is placed at the entrance pupil of an objective lens, which is easy to realize in a microscope system.

2.1 Pupil-filter design

Based on scalar focusing method, the lateral normalized intensity distribution in the focal plane of a 3-blet phase-only pupil-filter is denoted as[12-13]

$$I(\rho,0)=\left|\frac{2}{\rho}\{J_1(\rho)-2[aJ_1(a\rho)-bJ_1(b\rho)]\}\right|^2$$

where $J_1(\rho)$ is the first-order Bessel function of the first kind, a and b are the normalized outer and inner radii of the pupil-filter, and ρ is normalized radial coordinates $\rho=(2\pi/\lambda)(\mathrm{NA})R$, with R denoting the genuine radial coordinates, and NA is the numerical aperture of the objective lens. The optimal value of a and b can be obtained through

$$\left.\frac{\partial^2 I(\rho,0)}{\partial\rho^2}\right|_{\rho=0}=0$$

To design a pupil-filter with NA greater than 0.6, a vector focusing method is preferred[14]. For an n-belt phase-only pupil-filter, the components of the field can be written as[15-17]

$$E_x=-\mathrm{i}A(I_0+I_2\cos 2\varphi)$$
$$E_y=-\mathrm{i}AI_2\sin 2\varphi$$
$$E_z=-2AI_1\cos\varphi$$

with

$$I_0=\int_0^\alpha\sqrt{\cos\theta}\sin\theta(1+\cos\theta)J_0(kr\sin\theta)\cdot\exp(\mathrm{i}kz\cos\theta)\mathrm{d}\theta$$
$$I_1=\int_0^\alpha\sqrt{\cos\theta}\sin^2\theta J_1(kr\sin\theta)\exp(\mathrm{i}kz\cos\theta)\mathrm{d}\theta$$
$$I_2=\int_0^\alpha\sqrt{\cos\theta}\sin\theta(1-\cos\theta)J_2(kr\sin\theta)\cdot\exp(\mathrm{i}kz\cos\theta)\mathrm{d}\theta$$
$$\alpha=\arcsin\mathrm{NA}$$
$$A=\pi l_0 f/\lambda$$

where φ is the azimuthal angle, k is the wave vector, J_0, J_1, and J_2 are the first kind Bessel functions in the zero, first and second orders, respectively.

2.2 Typical geometrical parameters

One of the state-of-the-art manufacturing technologies to produce micro-optics is UV-LIGA[18]. During the manufacturing process, the alignment accuracy determines the relative position between micro-structures; the limited size of light spot brings in quantization error in edges, and the resulted apex angle can scatter incident light, reducing the efficiency of products due to diffraction[19]. Optical proximity effects occur, one result of which is to smooth the sharp edges[20].

In consideration of the primary types of fabrication errors in practice, four parameters are adopted. The schematic graph about the eccentricity and deflection angle is shown in Fig. 1(a). For simplicity, the center of the n-th belt of an n-belt pupil-filter is set as origin O in the polar coordinates system. The line passing through the center of the first-belt O_1 and O is set as the polar axis. The radius of the n-th belt is normalized to be 1, and the radius of the k-th belt is termed as r_k. Thereby the center of the k-th-belt is biased from O with a normalized distance of ρ_k and a deflection angle of θ_k. It should be clarified that $\theta_1=0$, and θ_k is between 0 and π. The rounding effect of boundary can be generated by the Gaussian filtering with a half window width of w, to smooth the profile of the pupil-filter, as shown in Fig. 1(b). Fig. 1(c) shows the belt with roundness caused by the positioning error of the fabrication system. Let the radial length of the actual belt be h_i. The roundness of the k-th belt can be expressed with root - mean - square value of the distance

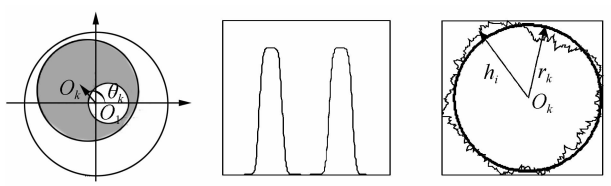

(a) Eccentricity and deflection (b) Rounding (c) Roundness

Fig. 1 Schematic graph for the profiles with fabrication errors

$$c_k=\sqrt{\frac{1}{n}\sum_{i=1}^{n}|h_i-r_k|^2}$$

2.3 Functional parameters

The intensity profiles of the Airy disk and super-resolution light pattern are shown in Fig. 2 and some functional parameters can be defined as

$$G=\frac{r_S}{r_D} \tag{2}$$

$$\text{Strehl}=\frac{S_{\max}}{D_{\max}} \tag{3}$$

$$M_k=\frac{I_k}{S_{\max}} \tag{4}$$

Here G is the radius at which the main lobe intensity of the super-resolved light pattern falls to half of the central intensity divided by the corresponding radius of the Airy disk. Strehl is the central intensity of super-resolved light pattern divided by that of the Airy disk[21]. M_k is the ratio between the peak intensity of the k-th sidelobe I_k and the central intensity for super-resolved light pattern $S_{\max}$.

In order to describe the intensity profile more completely, the valley intensity of the k-th order L_k is also recorded.

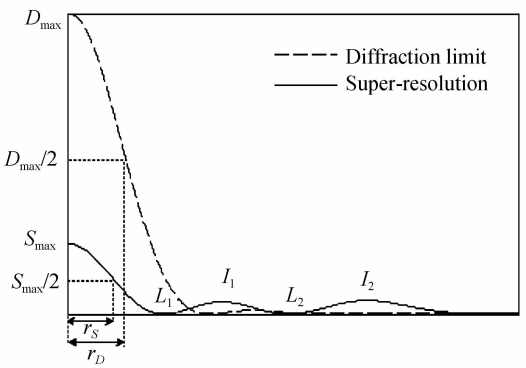

Fig. 2 Intensity profiles

3 Results and discussion

The structured surfaces with fabrication errors are modeled with MATLAB, and the output optical field of the pupil-filters is traced by VirtualLab. The wavelength of the light source is 632.8 nm. The effects of the fabrication errors listed above are analyzed on a 3-belt phase-only pupil-filter with the normalized radii $r_1=0.28$ and $r_2=0.5575$[14]. The focal length and pupil diameter of the objective lens are 160 mm and 6 mm, respectively. Thereby the theoretical distinguishing distance 20.5871 μm can be obtained using Eq. (1). Additionally, under the condition of $K=15\%$, the system′s Rayleigh distance is 21.1596 μm without pupil-filter, and the super-resolved distinguishing distance is 16.17 μm.

3.1 Eccentricity and deflection angle

Due to the asymmetry of the pupil-filter, the symmetry of the output light pattern is checked by comparing the minimum and maximum values on the contour with the peak intensities in the first-order sidelobe. Fig. 3 shows their difference in the normalized intensities ranging between 0.001 0 and 0.046 1, where the x and y coordinates stand for ρ_1 and ρ_2, respectively, ranging between 0 and 0.06.

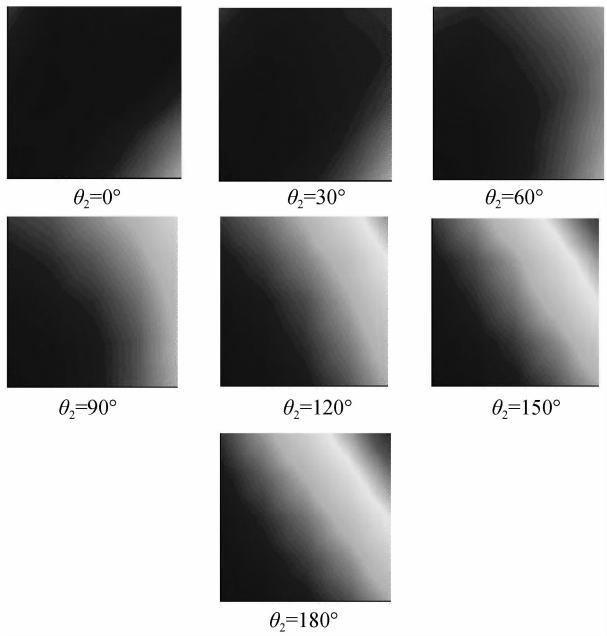

Fig. 3 The intensity difference for different ρ_1, ρ_2 and θ_2

It is obvious that the difference is getting larger as ρ_1, ρ_2 and θ_2 increase, indicating the deterioration of symmetry of the output field. Here the imaging resolution is determined by the worst direction of the light field.

Table 1 shows the correlation coefficients between the geometrical parameters and the super-resolution factors, where the absolute values of correlation coefficients are classified into 5 levels as noted. The eccentricity of the outer belt ρ_2 influences G and Strehl more significantly than the inner belt ρ_1 does, and the deflection angle has a weak influence. As a result ρ_2 is a significant parameter to be specially considered in quality control.

Table 1 Correlation coefficients of eccentricity and deflection

	ρ_1	ρ_2	θ_2
G	0.016 6	0.899 2	0.163 5
Strehl	−0.150 3	0.848 5	0
M_1	0.277 6	0.437 0	0.517 7
M_2	−0.303 6	0.247 4	−0.021 7

Note:

- 0.80-1.00 very strong
- 0.60-0.79 strong
- 0.40-0.59 moderate
- 0.20-0.39 weak
- 0.00-0.19 very weak

3.2 Rounding

The difference between the minimum and maximum intensities shown in Fig. 4 in solid line is very small, indicating that the output field has good symmetry. Since the rounding is set to test the super-resolution, the changing rates of the functional factors are calculated as well, as shown in Table 2.

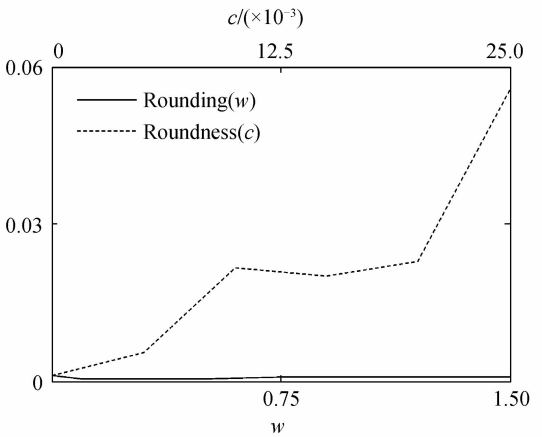

Fig. 4 The intensity difference for rounding and roundness

Table 2 The effect of rounding

	G	Strehl	M_1	M_2
Correlation coefficient	0.974 7	0.891 5	0.927 1	−0.986 2
Rate of change/%	10.47	17.80	29.04	9.41

3.3 Roundness

The intensity difference is illustrated as a dotted line in Fig. 4. It is evident that the light field is not symmetric under the fabrication error roundness. As the roundness, eccentricity and deflection angle cause asymmetry to the topography of the pupil-filter, while the pupil-filter is still perfectly symmetric accompanied with the error rounding. It is the symmetry of the pupil-filter that affects the light pattern directly. The correlation coefficients and changing rates of the super-resolution parameters are shown below.

Table 3 The effect of roundness

	G	Strehl	M_1	M_2
Correlation coefficient	0.908 5	0.838 5	−0.881 9	−0.060 1
Rate of change/%	1.29	0.34	16.87	6.88

Obviously the rounding affects the super-resolution behavior more significantly than the roundness.

3.4 The 5-belt and 7-belt pupil-filters

As demonstrated in the 3-belt pupil-filter, the eccentricity of the second belt has greater influence on super-resolution than the first belt. Now the relative significance of different belts is also investigated for the 5-belt[6] and 7-belt[14] phase-only pupil-filters. The normalized intensity profiles with different eccentric distances on the first and (n-1)th belts for the n-belt pupil-filter are presented in the upper and lower rows of Fig. 5, respectively. Fig. 6 shows the values of the valley intensity L_1 and radius G. The captions (a), (b), (c) stand for 3-belt, 5-belt and 7-belt pupil-filters, respectively.

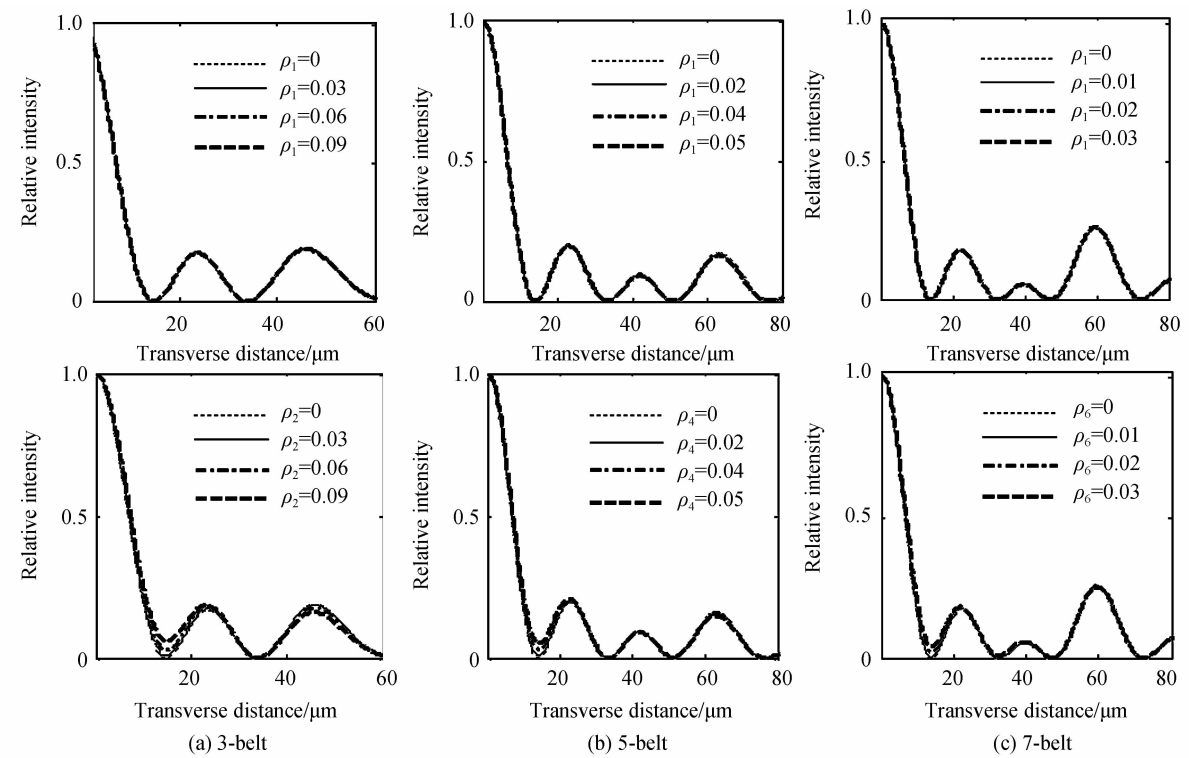

Fig. 5 Intensity profiles with eccentricity

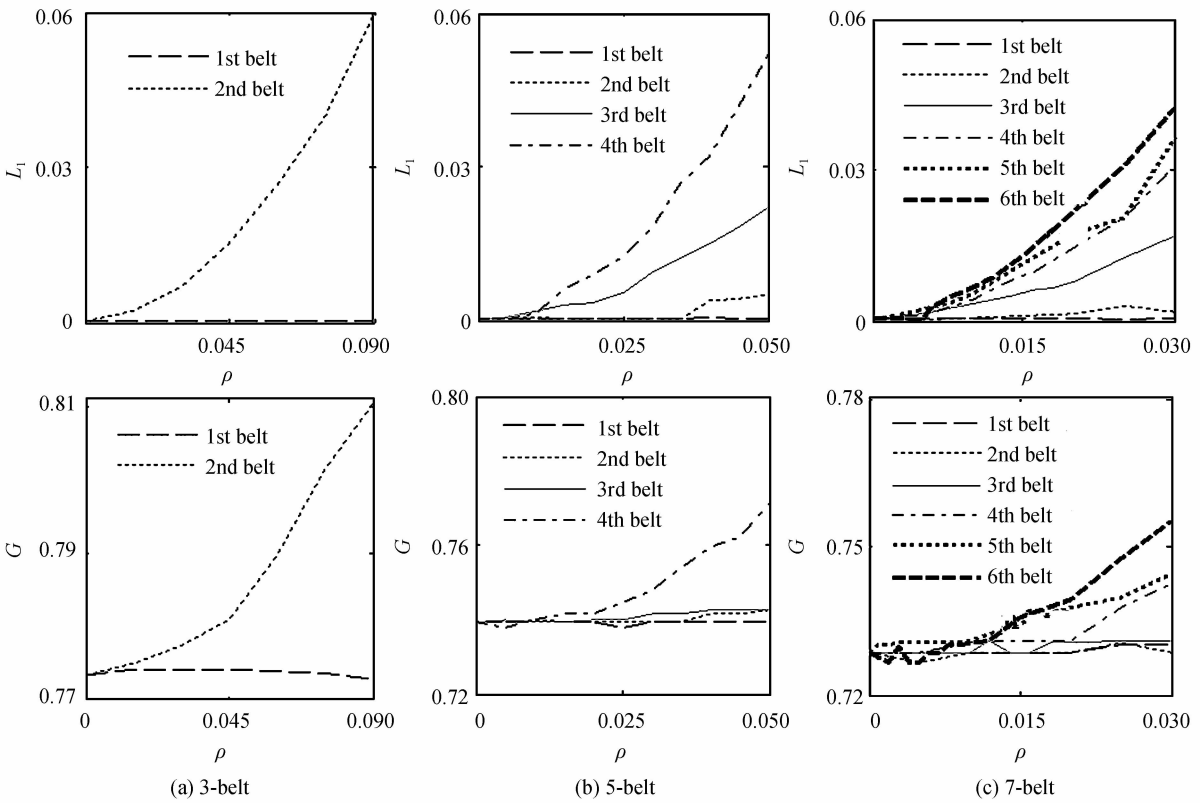

Fig. 6 L_1 and G with eccentricity

With the eccentricity and the order of the pupil-filter belt increasing, L_1 is getting greater as well, which causes the expansion of the mainlobe, thus leading to the decline of super-resolution ability. Thereby the quality of the outer belt influences super-resolution property more severely. In another word, the eccentricity of the outer belt needs to be controlled with tighter tolerance than the inner belts.

4 Conclusions

From the detailed analysis it can be concluded that the geometrical parameters eccentricity and rounding can be determined as the function-oriented geometrical parameters. Besides, the eccentricities of the outer belts need to be controlled more tightly than the inner belts. It is demonstrated that this method of quality control for pupil-filter is versatile, thus it can be applied to determine the design specifications of other micro- structured elements.

References

[1] ZAPPE H. Fundamentals of micro-optics[M]. Cambridge University Press, 2010.

[2] SULESKI T J, KATHMAN A D, PRATHER D W. Diffractive optics: design, fabrication, and test [M]. Bellingham, WA: Spie Press, 2004.

[3] International Organization for Standar-dization. ISO 25178-2: Geometrical product specifications (GPS): surface texture: areal—part 2: terms, definitions and surface texture parameters[S]. 2012.

[4] LUO Hong-xin, ZHOU Chang-he. Comparison of superresolution effects with annular phase and amplitude filters [J]. *Applied Optics*, 2004, **43**(34): 6242-6247.

[5] ZHAO Wei-qian, QIU Li-rong, FENG Zheng-de. Effect of fabrication errors on superresolution property of a pupil filter [J]. *Optics Express*, 2006, **14**(16): 7024-7036.

[6] LIU L, DIAZ F, WANG L, *et al*. Superresolution along extended depth of focus with binary-phase filters for the Gaussian beam [J]. *Journal of the Oriental Society of Australia A*, 2008, **25**(8): 2095-2101.

[7] WECKENMANN A, HARTMANN W. Function-oriented method for the definition and verification of microstructured surfaces[J]. *Precision Engineering*, 2013, **37**(3): 684-693.

[8] HARTMANN W, WECKENMANN A. B6. 1-function-oriented dimensional metrology-more than determining size and shape[C]. Proceedings SENSOR, 2013, **2013**: 285-290.

[9] HARTMANN W, WECKENMANN A. Verifying the functional ability of microstructured surfaces by model-based testing[J]. *Measurement Science and Technology*, 2014, **25**(9): 094012.

[10] MYERS J L, WELL A, LORCH R F. Research design and statistical analysis[M]. Routledge, 2010.

[11] RAYLEIGH L. XII. On the manufacture and theory of diffraction-gratings [J]. *The London, Edinburgh, and Dublin Philosophical Magazine and Journal of Science*, 1874, **47**(310): 81-93.

[12] WANG Hai-feng, GAN Fu-xi. High focal depth with a pure-phase apodizer[J]. *Applied Optics*, 2001, **40**(31): 5658-5662.

[13] WANG Hai-feng, GAN Fu-xi. Phase-shifting apodizers for increasing focal depth[J]. *Applied Optics*, 2002, **41**(25): 5263-5266.

[14] WANG Hai-feng, SHEPPARD C J R, RAVI K, *et al*. Fighting against diffraction: apodization and near field diffraction structures[J]. *Laser & Photonics Reviews*, 2012,

6(3): 354-392.

[15] WANG Hai-feng, SHI Lu-ping, YUAN Gao-qiang, *et al*. Subwavelength and super-resolution nondiffraction beam[J]. *Applied Physics Letters*, 2006, **89**(17): 171102-171102-3.

[16] RICHARDS B, WOLF E. Electromagnetic diffraction in optical systems. II. Structure of the image field in an aplanatic system[J]. *Proceedings of the Royal Society of London. Series A. Mathematical and Physical Sciences*, 1959, **253**(1274): 358-379.

[17] BOIVIN A, WOLF E. Electromagnetic field in the neighborhood of the focus of a coherent beam[J]. *Physical Review*, 1965, **138**(6B): B1561.

[18] SAILE V. LIGA and its Applications[M]. John Wiley & Sons, 2009.

[19] SOIFER V A. Methods for computer design of diffractive optical elements[M]. John Wiley & Sons, Inc. 2001.

[20] KAHNG A B, ROBINS G, SINGH A, *et al*. Filling algorithms and analyses for layout density control[J]. *Institute of Electrical and Electronics Engineers Transactions on Computer-Aided Design of Integrated Circuits and Systems*, 1999, **18**(4): 445-462.

[21] SALES T R M, MORRIS G M. Diffractive superresolution elements[J]. *Journal of the Oriental Society of Australia A*, 1997, **14**(7): 1637-1646.